REPORT DOCUMENTATION PAGE

AFRL-SR-AR-TR-03-

0229

1. AGENCY USE ONLY *(Leave blank)*	2. REPORT DATE	3. REPC
	5-NOV-2002	FINAL (OCT 1998 - SEP 2002)

4. TITLE AND SUBTITLE
SMART MESOFLAPS FOR AEROELASTIC TRANSPIRATION TO CONTROL SHOCK BOUNDARY LAYER INTERACTIONS

5. FUNDING NUMBERS
F49620-98-1-0490

6. AUTHOR(S)
PROFESSOR ERIC LOTH

7. PERFORMING ORGANIZATION NAME(S) AND ADDRESS(ES)
UNIVERSITY OF ILLINOIS
DEPARTMENT OF AERONAUTICAL & ASTRONAUTICAL ENGINEERING
306 TALBOT LABORATORY, MC-236
104 SOUTH WRIGHT STREET
URBAN, IL 61801-2935

8. PERFORMING ORGANIZATION REPORT NUMBER

9. SPONSORING/MONITORING AGENCY NAME(S) AND ADDRESS(ES)
AFOSR/NA
4015 WILSON BOULVARD
ARLINGTON, VA 22203

10. SPONSORING/MONITORING AGENCY REPORT NUMBER

11. SUPPLEMENTARY NOTES

12a. DISTRIBUTION AVAILABILITY STATEMENT

Approved for public release;
distribution unlimited.

12b. DISTRIBUTION CODE

13. ABSTRACT *(Maximum 200 words)*

The grant investigated a new concept in shock-wave/boundary-layer interaction control: the use of aeroelastic mesoflaps to provide efficient recirculation transpiration. Appendix 1A presents a set of Power-Pont slides which summarize the major finding of the study and also suggest a potential path forward to develop the technology and transition it to allow a bleedless supersonic inlet. As such, the goal would be to allow the overall benefits of a zero-bleed boundary layer control system into supersonic aircraft inlets: via retrofitting current inlets (e.g. the F-18E/F) or incorporating into design of future aircraft (e.g. the Long Range Strike Aircraft). As noted on Slide 2, the advantages of a bleedless inlet as evaluated by the aircraft industry are substantial and can considered in terms of either extended range (as much as 20%) or reduced gross take-off weight (as much as 10% as detailed in Part 7). As discussed on slides 2-9, the aerodynamic benefits for the mesoflaps over conventional recirculation transpiration with a porous plate include improved aerodynamics for subsonic conditions, more aerodynamic aerodynamic bleed and injection for shock interactions and increased shock stability. These benefits have been quantified for oblique impinging shocks, ramp-generated oblique shocks and normal shocks (Part 2). Additional research was conducted to understand the structural dynamic issues (Parts 3 and 4) and how a closed-loop control system might be employed in order to allow further performance increases (Part 5). Appendix 1B gives an overview of the how these various research activities were integrated together.

14. SUBJECT TERMS

15. NUMBER OF PAGES
21

16. PRICE CODE

17. SECURITY CLASSIFICATION OF REPORT	18. SECURITY CLASSIFICATION OF THIS PAGE	19. SECURITY CLASSIFICATION OF ABSTRACT	20. LIMITATION OF ABSTRACT
UNCLASSIFIED	UNCLASSIFIED	UNCLASSIFIED	

UNIVERSITY OF ILLINOIS
AT URBANA-CHAMPAIGN

NOV - 5 2002

Department of Aeronautical and Astronautical Engineering

306 Talbot Laboratory, MC-236
104 South Wright Street
Urbana, IL 61801-2935 USA

November 1, 2002
(217) 244-5581

Dr. Tom Beutner
AFOSR/NA
801 North Randolph, Room 732
Arlington, VA 22203-1977

Dear Dr. Beutner,

Please find enclosed an MS Word copy of the final report for the following grant: F49620-98-1-049 covering the period October 1998 - September 2002. In addition, a soft copy of all the appendix material in PDF form is included in this zip disk. Please let me know if any part of this report needs to be modified with respect to DARPA clearance and do not hesitate to contact me for clarification or further information/detail. Once clearance has been given, please also let me know how many hard and or soft copies you would like of this report.

With best regards,

Eric Loth, Ph. D.
Professor of Aeronautical
and Astronautical Engineering

cc: Dr. Steve Walker, Dr. Jim Pittman, Mr. Skip Gridley, and Mr. Matt Tallent

telephone 217-333-2651 • *fax* 217-244-0720 • *url* http://www.aae.uiuc.edu

FINAL REPORT

Smart Mesoflaps for Aeroelastic Transpiration to Control Shock Boundary Layer Interactions

Grant Number: F49620-98-1-049
Grant Period: July 1998 - March 2002

The principal investigators include: Prof. Andrew Alleyne, Prof. Craig Dutton, Prof. Philippe Geubelle, Prof. E. Loth*, Prof. Dan Tortorelli, and Prof. Scott White (of the University of Illinois); Dr. Jim Mace and Dr. Fred Roos (of Boeing); as well as Dr. Dave Davis (of NASA Glenn Research Center).

The reports discuss highlights of the effort under the DARPA Micro-adaptive Flow Control Program (MAFC) for an AFOSR grant to the University of Illinois, which included a sub-contractual arrangement with Boeing through the Phantom Works organization as well as partnership with NASA Glenn Research Center and the NASA Langley Research Center (with sponsorship via the UEET program).

*Aeronautical & Atronautical Engineering Department, 104 S. Wright St, Urbana IL, University of Illinois at Urbana-Champaign, (217) 244-5581, e-loth@uiuc.edu

Contents

Part 1:
Synopsis of Overall Research

The grant investigated a new concept in shock-wave/boundary-layer interaction control: the use of aeroelastic mesoflaps to provide efficient recirculation transpiration. As such, the goal would be to allow the overall benefits of a zero-bleed boundary layer control system into supersonic aircraft inlets: via retrofitting current inlets (e.g. the F-18E/F) or incorporating into design of future aircraft (e.g. the Long Range Strike Aircraft). The advantages of a bleedless inlet as evaluated by the aircraft industry are substantial and can considered in terms of either extended range (as much as 20%) or reduced gross take-off weight (as much as 10% as detailed in Part 7). The aerodynamic benefits for the mesoflaps over conventional recirculation transpiration with a porous plate include improved aerodynamics for subsonic conditions, more aerodynamic aerodynamic bleed and injection for shock interactions and increased shock stability. These benefits have been quantified for oblique impinging shocks, ramp-generated oblique shocks and normal shocks (Part 2). Additional research was conducted to understand the structural dynamic issues (Parts 3 and 4) and how a closed-loop control system might be employed in order to allow further performance increases (Part 5).

To translate and demonstrate these advantages into a inlet-type flowfield, a Mach 2 research inlet was designed and fabricated for the NASA Unitary wind tunnel. Testing with solid-wall condition, several bleed geometries, and two mesoflap geometries was conducted during the spring and summer of 2002 in order to asses the mesoflap performance. In particular, it was desired that the mesoflap performance not only exceed that of the solid-wall condition (in terms of stagnation pressure recovery, flow steadiness, and flow uniformity) but also approach that of the best bleed condition while *simultaneously* eliminating any bleed-drag effects. Comparisons with passive porosity (PASSPort) were also conducted by NASA Langley researchers and will be discussed in a separate NASA report. In general, performance above the solid-wall condition and also in some cases similar to the best bleed condition was demonstrated at the highest Reynolds numbers tested (Re=3x106/ft) at zero degrees angle of attack.

Part 2 of this study gives some details on the aerodynamic performance of the mesoflaps in the UIUC wind tunnel configuration for several conditions and shows that positive overall benefits were demonstrated for this fundamental flow physics. Part 3 of this study shows that the aeroelastic response of the mesoflaps is non-linear and is investigated both in terms of steady-state deflections as well the unsteady response for a single-flap system. Part 4 of this report discusses the experimental testing conducted to detail the transformation characteristics and the fatigue life of the nitinol mesoflaps. Part 5 discusses the investigations to allow-closed-loop control of the devices. Part 6 summarizes the Unitary wind tunnel test to investigate a more realistic inlet flow. Finally, Part 7 documents the system-level analysis investigated to determine the net effect on aircraft performance for inclusion of a bleedless inlet technology, such as that which may be provided with mesoflaps.

Part 2:

UIUC Wind Tunnel Experiments and Fixed-Deflection Simulations

Both impinging oblique and normal shock/boundary layer interactions with mesoflap control have been investigated experimentally in the University of Illinois at Urbana-Champaign gas-dynamics flow facilities, as well as numerically in the same flow facilities, using pre-set fixed deflections (note: the simulations which describe the aero-elastic behavior are discussed in Part 3).

In the experiments, several thicknesses of both Nitinol and aluminum arrays of several geometric designs have been studied. In addition, interactions of the shock waves with solid walls (no control) and with a conventional porous plate (macro-porous plate) have been examined as baselines for comparison. The experimental methods used to examine and characterize the control effectiveness of the mesoflap systems include: schlieren/shadowgraph photography, surface flow visualization, mean and fluctuating wall static pressure, mean and fluctuating pitot pressure, mean velocity and turbulence moments from laser Doppler velocimetry (LDV), and skin friction determined from the laser interferometer skin friction (LISF) method. In general, the results showed that the mesoflaps were able to increase the stagnation pressure recovery and flow stability as compared to a solid-wall base-line. In addition, the cases with an impinging oblique shock were also able to reduce the overall boundary layer and displacement thickness as well.

The numerical investigations examined a large range flow geometries including the parametric study of flap numbers, flap deflections, flap positions, cavity depth, Mach number, etc. As in the experiments comparison was made to both solid-wall cases as well as to conventional macro-porous plates (with span-wise slots). The numerical technique employed was predominately a two-dimensional Reynolds-Averaged Navier-Stokes solver, although some three dimensional simulations were completed as well. Performance indicators included mass-averaged stagnation pressure distributions and boundary layer characteristics (thickness, displacement thickness, shape factor, etc). The simulations indicated that the upstream deflections were key to allowing significant "λ-effect" benefits, while the downstream flaps were key to rehabilitating the boundary layer. In both normal-shock and ramp-generating shock cases, as the boundary deflections increases, the overall stagnation pressure recovery tended to increase, but at high values of the deflections the system yielded significantly thicker downstream boundary layers. Notably, the magnitude of the optimum deflections (good pressure recovery for nominal boundary layer degradation) were on the order of 2-5 displacement thicknesses for the M=2+ oblique shock cases but only about ½ of a displacement thickness for the M=1.4 normal-shock cases.

With respect to both the experiments and the simulations, recommendations for further studies would be to examine the details of the unsteady and especially three-dimensional fluid physics near and around the mesoflap interactions. Also, investigation of new mesoflap concepts which are more three-dimensional, i.e. which create strong stream-wise vorticity both upstream and downstream of the interaction may allow even further performance benefits.

Many conference papers have been presented which document these experimental studies of mesoflap control of SBLIs over the course of this four-year study. In addition, several refereed journal articles are either currently in press or are in various stages of review or preparation. Two UIUC M.S. theses describe in detail these studies (Hafenrichter, Gefroh) with two more in the final stages of preparation (Jaiman, Orphanides).

Part 3:
Aeroelastic Simulations

In this part of the project, aeroelastic simulations have been performed with two distinct objectives in mind. The first one has been to study numerically the steady-state response of the mesoflap system. This project has been the topic of B. Wood's M.S. thesis (Wood, 1999) and has been summarized in a paper (Wood *et al.*, 2000). As indicated in these studies, the numerical method used in this steady-state analysis relies on an iterative coupling scheme between an unstructured fluid solver (NSU2D) and an in-house static finite element solver. On the numerical side, a major emphasis has been placed on introducing specially adapted criteria to speed up the convergence of the aeroelastic code. A typical result derived from this work is shown in Figure 1, which presents the Mach number distribution in the inlet and in the cavity for an 8-flap system and clearly illustrates the aeroelastic deformation of the flaps and the associated recirculation.

The second part of the aeroelastic modeling project has focused on time-resolved simulations of the dynamic response of the mesoflap system. This study has so far been limited to the fundamental problem of a single flap placed above a rectangular cavity and subjected to a supersonic flow. The simulations have been performed with an in-house explicit aeroelastic code involving an unstructured finite volume fluid solver that incorporates a robust mesh adaptivity scheme, and an unstructured finite element solver (Geubelle *et al.*, 2001). Figures 2 and 3 respectively show a typical time sequence of the pressure and velocity distributions in the vicinity of the single-flap system.

Figure 4 presents the dynamic response of a 200 (left figure) and 400 μm thick (right figure) flap for the Ma=2 case. This result illustrates how the flap thickness strongly affects the response of the system, which evolves from a state of sustained oscillations (i.e., flutter) for the thinner flap case to a stable state with vanishing oscillations for the thicker flap case.

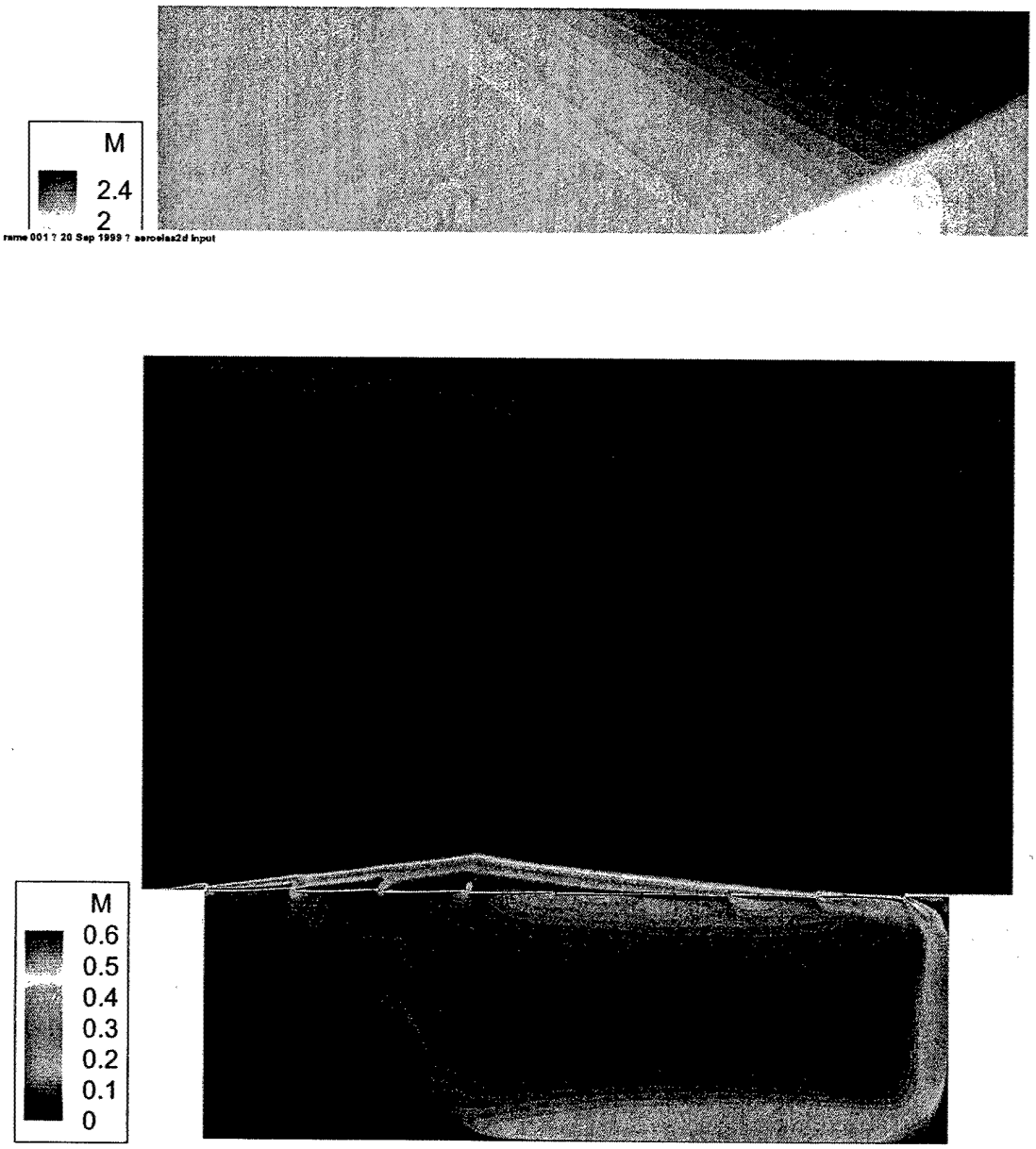

Figure 1. Steady-state aeroelastic simulation: Mach contours in the main inlet flow (top) and resolved in the cavity (bottom).

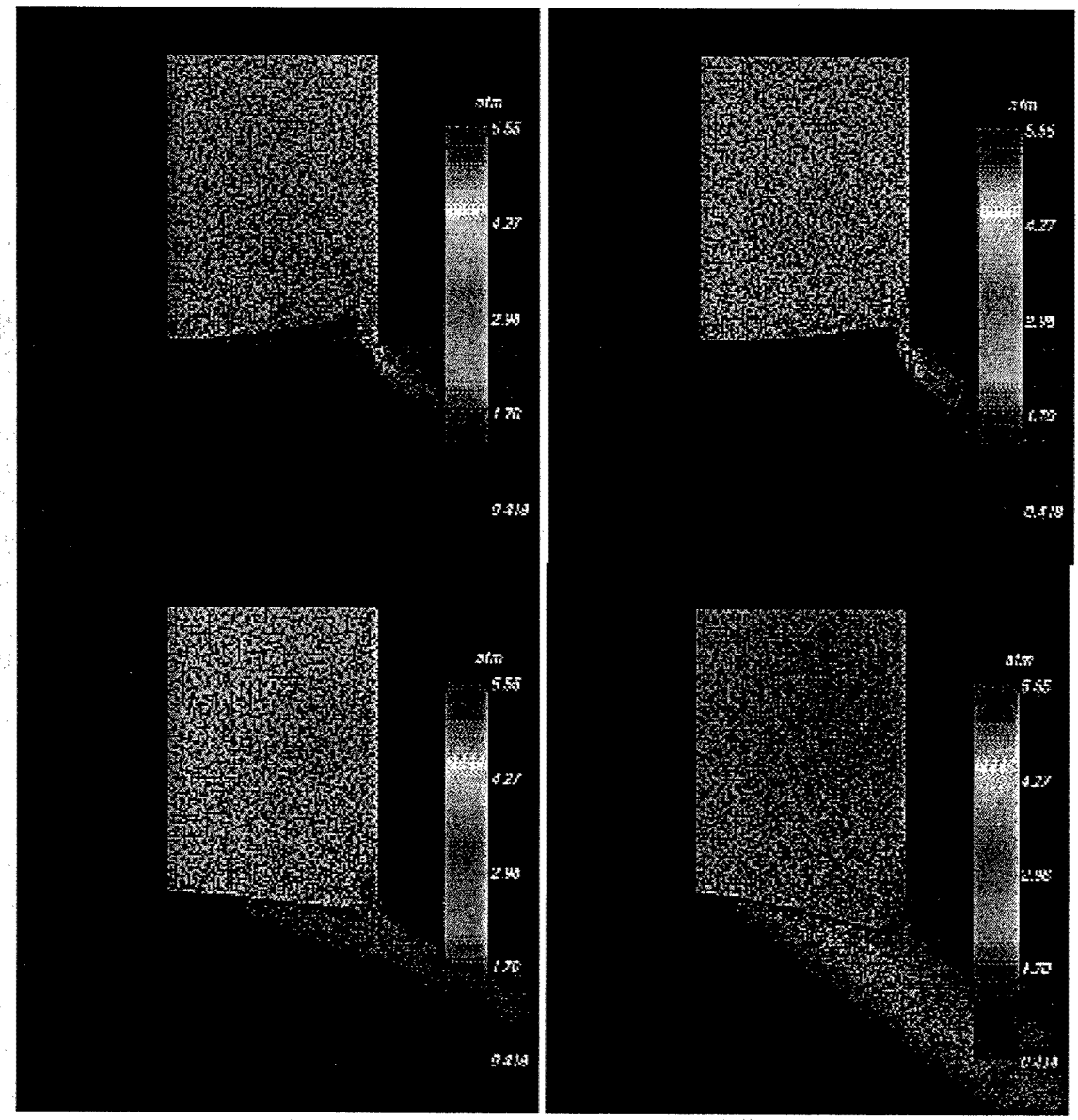

Figure 2. Evolution of the pressure distribution in the vicinity of an aeroelastically deforming 200 μm thick flap, showing the ability of the dynamic aeroelastic code to capture the complex compression and expansion events during the flap deformation cycle.

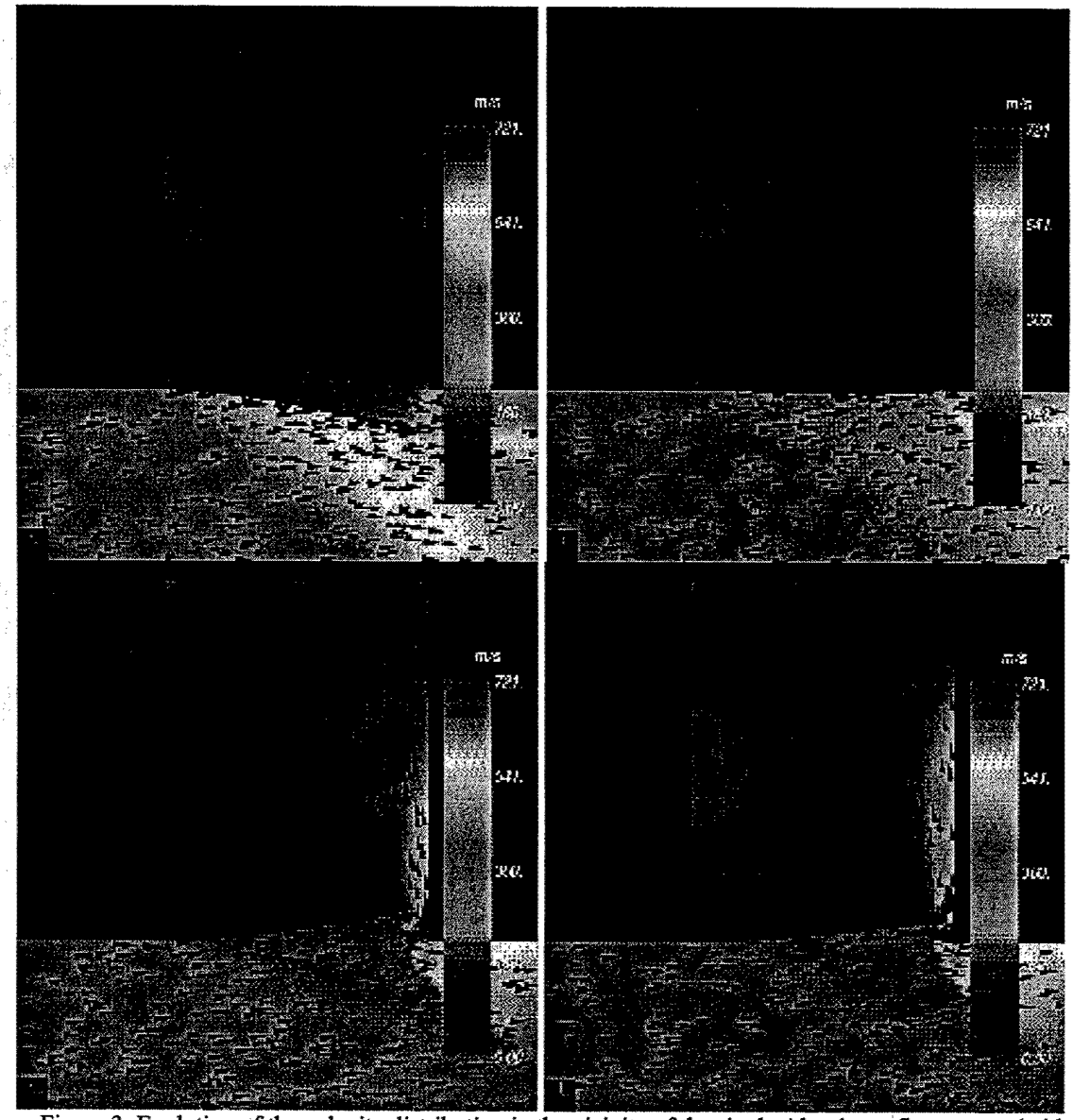

Figure 3. Evolution of the velocity distribution in the vicinity of the single Aluminum flap system (with a flap thickness of 200 μm) showing the recirculation taking place in the cavity.

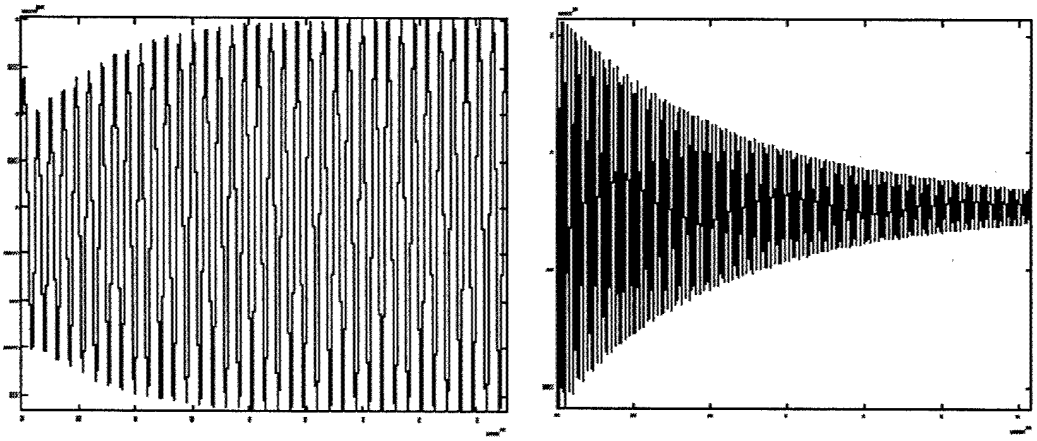

Figure 4. Dynamic response of a 200 (left) and 400 μm thick (right) flap: evolution of the flap tip deflection (in m) versus time (in s).

A detailed parametric study has been conducted to quantify the effects of the gap size, cavity depth and flap thickness on the flutter response of the system. A typical result is shown in Figure 5, which presents the dependence of the Mach number and flap thickness on the (non-dimensionalized) steady-state amplitude of the flap oscillations. The transition from a stable (non-oscillating) response to a fluttering regime characterized by a finite amplitude is clearly visible in the 300 μm case. The decrease of the amplitude with respect to the Mach number observed in the 200 μm case is due to the fact that the dynamic pressure is used in the non-dimensionalization of the amplitude: the actual steady-state amplitude reaches a plateau at higher Ma values.

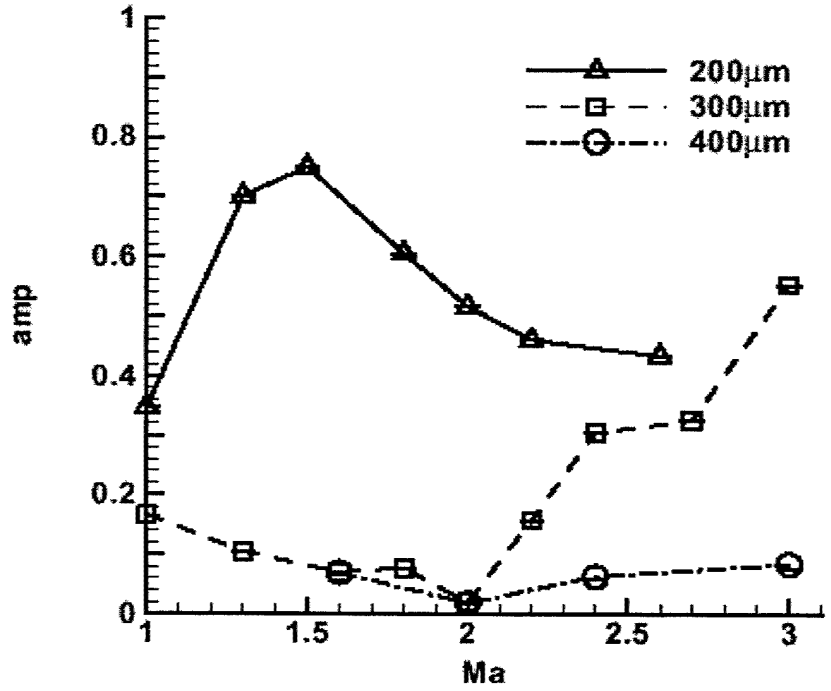

Figure 5. Effect of the Mach number and the flap thickness on the (non-dimensional) steady-state amplitude of the flap tip deflection.

This dynamic aeroelastic study is the topic of L. Ozhkaya's M.S. thesis which will be completed in the next few months and will also contain the simulation of a 2-flap system more relevant to the SMART set-up.

References

Geubelle, P. H., Huang, C., Fiedler, R., Breitenfeld, M. S. and Haselbacher, A. (2001) "Simulation of dynamic fracture events in solid propellant rockets". 37th AIAA/ASME/SAE/ASEE JPC Conference and Exhibit, July 8-11, 2001. Paper AIAA 2001-3953.

Wood, B. (1999) "Aeroelastic Simulation of a Novel Transpiration System", M.S. Thesis, Dept. of Aeronautics & Astronautics, Univ. of Illinois at Urbana-Champaign.

Wood, B., Loth, E. and Geubelle, P. H. (2002) "A numerical methodology for an aeroelastic supersonic viscous flow". To appear in *J. Fluid and Structures*.

Part 4:
Smart Materials Characterization

The use of shape memory alloys (SMA) in SMAT is critical to the success of this approach to SBLI. In support of this research a comprehensive investigation of SMA material behavior and design of SMA flaps was undertaken in three focus areas [i-iii]. These focus areas included design/manufacturing, thermomechanical behavior, and fatigue response and are discussed in more detail in Refcs: A, B, and C.

i. Design and Manufacturing

Shape memory alloys exhibit a solid state transformation of material phase that gives rise to a highly nonlinear and hysteretic stress-strain response. A great deal of work has focused on describing their constitutive response under a variety of multidimensional loading conditions. Once an appropriate constitutive model is identified, the challenge is to incorporate the model and the complex response it describes into a design tool. Our approach was to utilize the standard finite element package ABAQUS for the design of SMA flaps. In addition to nonlinear analysis, ABAQUS features user-defined subroutines that we utilized to describe the constitutive response of Nickel-Titanium (NiTi) shape memory alloy. This subroutine was obtained from Prof. D. Lagoudas at Texas A&M University and calibrated for the material systems used at the University of Illinois. The fully integrated code was used to investigate design features (flap thickness, length, width, spacing, support material, etc.) of the flap system and their relative importance on flap performance. Flap thickness was found to be the single most important geometric parameter in the design process and the finite element results guided the evolution of five design generations of the flap system.

The FEA was also used to investigate the failure of early generations of the flap system in which high stresses led to material failure. In Fig. 1 the von Mises stress contours around the edge of a NiTi flap is shown under normal operating conditions (uniform pressure of 27.6 kPa). The stress concentration at the root of the notch on the edge of the flap indicates that material failure will initiate in this region as was confirmed in wind tunnel testing. A redesign of the flap featuring a scalloped edge that blends the flap into the central region alleviated this stress concentration and no further failures of this type occurred.

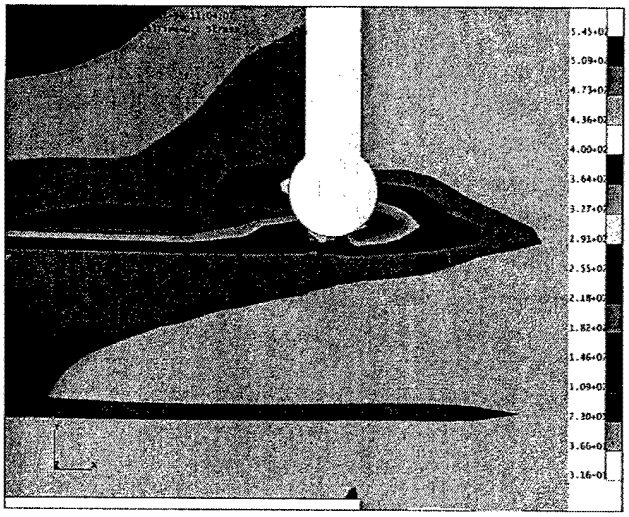

Fig. 1. von Mises stress contour around the notch tip of the relief cut for the NiTi flap showing stress concentration at the notch tip.

Manufacturing of the flap system was accomplished by Electric Discharge Machining (EDM) of the flaps from sheet stock of NiTi of the appropriate thickness. The sheet with

flaps cut out was then bonded onto a steel stringer plate to provide structural support. The combined flap/stringer assembly was then ready to be incorporated into a recirculation cavity and integrated into an inlet model and/or wind tunnel chambers. The effects of EDM manufacturing on NiTi behavior was investigated by Scanning Electron Microscopy (SEM) of the machined surfaces and compared to normal metal cutting processes and as-received material conditions. EDM was found to yield a much cleaner machined surface in which the affects of machining were limited to a surface region of a few microns. Some evidence of melting/recrystallization was evident, although no affects on mechanical behavior could be detected.

ii. Thermomechanical Characterization

Materials for SMAT testing were obtained from two independent suppliers: Shape Memory Applications (San Jose, CA) and, Special Metals Corporation (New Hartford, CT). Both superelastic and two higher temperature alloys were used. Full thermomechanical characterizations were carried out on all material types using Dynamic Mechanical Analysis (DMA) and Differential Scanning Calorimetry (DSC). DSC was used to obtain transformation temperatures and transformation enthalpies. The effects of various heat treatment conditions and processing methods on material behavior was analyzed by DSC. DMA provided mechanical properties as a function of temperature and loading frequency and was also used to investigate processing and heat treatment effects. Table 1 shows the full material properties that were obtained for the two primary material systems utilized in SMAT testing.

Table 1. DSC and DMA Results for NiTi Flap Materials

Property	H-SMA [49.32Ni-50.68Ti]		S-SMA [50.78Ni-49.22Ti]	
	as-received	800°C annealed	as-received	800°C annealed
M_s (°C)	55.8	65.6	--	5.0
M_f (°C)	52.0	62.8	--	-12.0
A_s (°C)	85.3	91.1	--	-8.0
A_f (°C)	97.4	105.0	--	12.0
ΔH_A (J/g)	25.0	27.1	--	--
ΔH_M (J/g)	17.7	29.1	--	--
E_A (GPa)	58.5	69.0	--	78.0
E_M (GPa)	41.0	46.8	--	53.0

iii. Fatigue Behavior of NiTi Flaps

Having designed the NiTi flaps for structural performance and aeroelastic efficiency, developed an efficient manufacturing technique for their fabrication, and fully characterized their thermomechanical behavior, our investigations moved to the fatigue response of NiTi flaps under a variety of load and environmental conditions. While the mass bleed/injection feature of SMAT is envisioned as a relatively low cycle phenomena over the lifetime of the engine, during certain operating conditions it was found that some of the flaps could experience flutter. These relatively small oscillations of flap position occur at high frequency and contribute to high cycle fatigue processes.

Our approach to the investigation of fatigue behavior was to test the actual flaps rather than a model test configuration. Fatigue lifetime is greatly influenced by boundary conditions and specimen geometry and as such, the most relevant testing is carried out on specimens that are as close to the actual design as possible. NiTi flaps were tested both in low amplitude strain (simulating operational conditions), and high amplitude strain (simulating overloads and resonant conditions). The results presented in Fig. 2 show that all NiTi materials tested possess greatly extended fatigue life compared to conventional structural alloys. It was also found that high temperature alloys with an A_f above the operational temperature show a much higher (about one order of magnitude) fatigue life in comparison to superelastic NiTi (with A_f below operational temperature). For the greatest fatigue life the operational temperature should be as far below the A_f transition as possible.

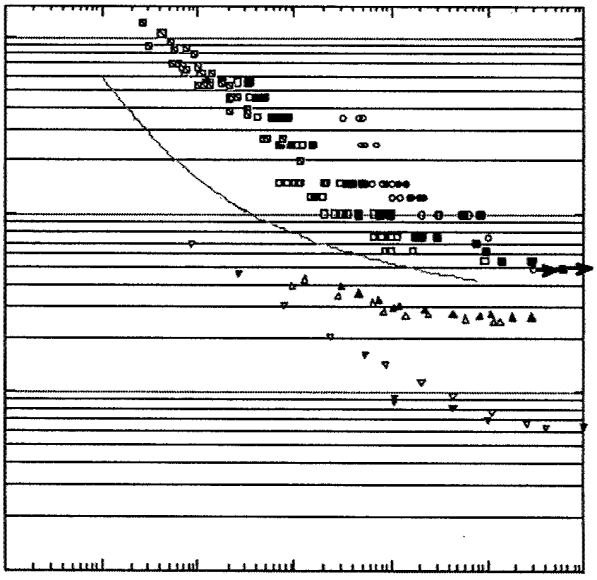

Fig. 2. *Comparison of fatigue response of sheet metal alloys.*

A. Krishnan, S. "Experimental characterization and finite element analysis of shape memory alloy flaps for aeroelastic transpiration," M.S. Thesis, Aeronautical and Astronautical Engineering, December, 2000.

B. Krishnan, S., Yoon, S.-H., and White, S.R. "Dynamic mechanical analysis of nitinol beams," Proceedings of the ASME 2000 International Mechanical Engineering Congress and Exposition, November 5-10, 2000, Orlando, FL, *Adaptive Structures and Materials Systems Symposium*, AD-Vol. 60, J. Redmond and J. Main, Eds., pp. 13-18.

C. Li, Q. "Structural behavior of nitinol micro flaps," Ph.D. thesis proposal, Aeronautical and Astronautical Engineering, October, 2002.

Part 5:
Mesoflap Control

The flap control portion of this research focused on the dynamic modeling and testing of the thermally activated smart material flap arrays. A dynamic model was developed that predicted the flap deflection as a function of power input. This model was verified on a benchtop test. Closed loop control strategies were developed and implemented via a digital controller on a benchtop test and in the UIUC wind tunnel. Benchtop tests provided promising results for tailoring flap aeroelastic behavior using different measurements. Excessive convective heat transfer posed fundamental limitations to achieving similar success in the UIUC wind tunnel. An overview of these aspects is given below with details provided in two M.S. theses (Tharayil & Crisman).

A detailed mechanistic model of the dynamic behavior of NiTi material under thermal power input was developed. This model incorporated heat transfer into the material, rate limits due to phase transformation dynamics, and mechanical deflections due to stiffness changes. The model was calibrated against data taken on a benchtop testbed developed at UIUC. Temperature and deflection data were used to verify the model's accuracy with very positive results.

A closed loop control was implemented on a benchtop testbed for controlling either cavity pressure or flap deflection. A simple PID feedback of flap deflection, measured by a laser sensor, or cavity pressure, measured by a static pressure transducer, was used as the baseline control strategy. This simple strategy was chosen because of the relatively long time constants associated with the thermal actuation mechanism. Two key modifications to the baseline PID were made. First, a hysteresis compensator was developed and implemented to account for a large amount of hysteresis present in the phase transformations between Martensite and Austenite phases. Secondly, a reference governor was developed to account for the limited power density achievable with commercial off the shelf heating actuation elements. The reference governor scheme is generalizable to any PID controlled system. The resulting control scheme was very effective in regulating any desired cavity pressure or flap deflection on the benchtop testbed used.

Tests were performed in the UIUC wind tunnel for both open and closed loop control of a flap array. The available power that could be put into the flaps could not be retained in the NiTi sufficiently to cause the necessary change in flap temperature. The convective heat transfer of the supersonic flow proved to be too great to allow any transformation from Martensite to Austenite. Even with insulation on the flaps and heating elements, it was not possible to raise the material temperature above the Austenite start temperature. The commercial, off-the-shelf heating elements were unable to provide the power densities necessary to overcome the large heat loss. Due to the challenges associated with thermally actuating the flap arrays, current efforts are targeting direct mechanical adjustment of flap deflections. Benchtop tests have been successfully completed and tests are currently underway in the UIUC wind tunnel.

Theses:

1) Crisman, P., "Modeling, Analysis, and Control of a Flap System for Shock Boundary Layer Interaction Control," M.S. Thesis, UIUC, 2000.
2) Tharayil, M., "Modeling and Control of a Smart Material Mesoflap System for Shock Boundary Layer Interaction Control," M.S. Thesis, UIUC, 2001.

Part 6:
NASA Langley Unitary Wind Tunnel Experiments

An essential element, from early in the program, was demonstration of the performance of SMART technology as replacement for conventional (aspirated) boundary-layer-control (BLC) bleed in a supersonic inlet. This demonstration was accomplished through a series of tests with a supersonic inlet model in Test Section 1 of the NASA Langley Research Center (LaRC) Unitary Plan Wind Tunnel (UPWT), a closed-circuit, continuous-flow, variable-density supersonic wind tunnel[R1].

Inlet performance testing was concentrated on Mach 2.0, the "design" Mach number of the inlet model, over the range $1.0 \times 10^6 \leq \text{Re/ft} \leq 5.0 \times 10^6$. The external-compression inlet was an existing two-dimensional UPWT inlet model[FR2] that had been reconfigured to simulate the shock-system geometry, and terminal normal-shock strength, representative of a vehicle flying at Mach 2.4. Mass flow rate through this inlet model was controlled by an opposing pair of remotely operated throttling flaps at the exit of the inlet. The compression ramp surfaces were fitted with interchangeable panels in the second-wedge and normal-shock-impingement regions. These panels were backed by cavities that could be vented to the tunnel flow outside the inlet. Porous panels provided aspirated BLC bleed (via the external venting), while installation of SMART panels (backed by unvented cavities) permitted evaluation of SMART BLC performance relative to conventional bleed. Principal instrumentation in the inlet model consisted of centerline arrays of static-pressure taps on the ramp and cowl surfaces, a 36-probe total-head rake located in the subsonic diffuser section of the inlet, and a pair of flush-mounted Endevco dynamic-response pressure transducers in the ramp surface at the rake station.

Inlet performance variables employed in evaluating SMART and other BLC configurations were **RECOV**, a weighted average of total pressures over a subset of the rake total-head probes; **DIST**, a simple (max-min) flow-distortion parameter; and $\mathbf{P'/P_0}$, the normalized rms wall-pressure unsteadiness at the rake station. The principal independent variable employed in the performance evaluations was the inlet mass flow ratio, $\mathbf{W_2/W_c}$, where W_2 is the estimated mass flow actually entering the inlet and W_c is the ideal, or "capture", mass flow. In cases of conventional-bleed BLC, the standard practice was adapted of adjusting W_2 to include the (approximated) bleed mass flow (not measured in these tests).

Performance of the inlet model in terms of the above parameters was evaluated (as a function of unit Re) for the solid-wall (i.e., no-bleed) case, the best of several conventional bleed cases, and two SMART cases (one using 0.0080 in thick aluminum flaps; the other employing Nitinol – a nickel-titanium "smart" alloy – flaps of 0.0094 in thickness). These SMART flap arrays were designed to a pressure loading corresponding to operation at Re = 3M/ft.

A pressure-recovery performance comparison at the SMART design shows that the SMART system nearly matches Bleed #1 (the best conventional-bleed configuration) in pressure-recovery improvement (over no bleed), particularly at the higher mass flow ratios. (It should be noted that the indication of mass flow ratios appreciably greater than one reveals the inadequacy of the simple approach that was taken to estimation of the inlet mass flow from the

total-head rake measurements. The estimation procedure provides sufficient relative, if not absolute, results.) In addition, the thinner aluminum SMART flaps were at least as effective as Bleed #1 in reducing flow distortion.

Since stability margin is a key figure of merit for supersonic inlets, the unsteady pressure results are significant in showing that the SMART panels displayed a larger stability margin than did conventional bleed. And the SMART panels exhibited a gradual degradation in shock stability, in contrast to the abrupt buzz transition shown by Bleed #1.

In summary, the SMART inserts produced recovery improvements (over bleed-free performance) without degradation of inlet flow uniformity or stability. At the SMART design condition, SMART nearly equaled the recovery characteristics of conventional bleed. Test data trends suggest that thinner, more-flexible SMART flaps would likely come closer to matching the recovery improvement shown by conventional bleed. All of which suggests that, with further tuning and optimization, SMART inlet BLC technology can meet conventional bleed performance characteristics while offering the weight-, drag-, and cost-reduction benefits derivable from elimination of BLC bleed.

R1. J.R. Micol, "Langley Research Center's Unitary Plan Wind Tunnel: Testing Capabilities and Recent Modernization Activities," AIAA Paper No. 2001-0456, January 2001.

R2. W.J. Monta and W.C. Sawyer, "Two-Dimensional Inlet Survey Model," unnumbered internal document prepared for NASA Langley Missile Peer Review Committee, May 1983.

Part 7:
System-Level Aircraft Performance for the LRSA

A preliminary trade study was undertaken in an effort to identify the potential benefit of incorporating SMART technology into a Long-Range Strike Aircraft (LRSA)-class flight vehicle.

The trade study involved Boeing LRSA conceptual vehicles of both Mach 2.4 and Mach 4.0 class. (The configurations are not presented here owing to export control and proprietary restrictions.) As configured, both LRSA vehicles are to be propelled by Pulsed Detonation Engines (PDE's), so the trade study initially evaluated potential payoffs from incorporating SMART shock/boundary-layer-interaction (SBLI) control into these PDE-powered concepts.

Although a Mach 4.0 vehicle was originally included in this SMART payoff analysis, emphasis was ultimately focused on the Mach 2.4-class LRSA vehicle, for several reasons. One was the consideration of the potential for application of SMART to the Quiet Supersonic Platform (QSP), a DARPA-sponsored effort to develop a multi-use, low-sonic-boom supersonic aircraft.

The Mach 2.4 LRSA vehicle studied is an uninhabited aircraft capable of delivering a 16,000-lb. payload, with a range of 6000 mi., and a 60,000-ft. altitude capability. The assumed mission profile involved supersonic cruise at altitude to 3000 mi., delivery of the 16,000-lb. payload, and supersonic cruise back to base.

Because the LRSA vehicles studied were conceptual, and therefore not fully designed and engineered, standard linear methods were utilized in the analysis. Also, for example, it was necessary to notionally define an inlet duct configuration for this study, to enable assessment of weights, volumes, etc. associated with the conventional-inlet-bleed baseline against which the SMART capability was to be compared.

The procedure employed was to define and size the baseline (bleed-equipped) vehicle, including the necessary fuel load to accomplish the mission. Then, assuming that SMART technology would provide inlet performance (i.e., pressure recovery, shock stability, etc.) equivalent to the conventional-bleed (baseline) case, the vehicle was resized and fuel load re-evaluated for the SMART-equipped vehicle.

Results showed that the principal SMART benefit (for the long, 6000-mi. LRSA mission range) accrued from SFC improvement associated with the lower drag of the SMART-equipped version (elimination of bleed drag $\rightarrow$ lower overall drag). The benefit was identified to be as much as 8% reduction in fuel burn. Converted into terms of life-cycle $ cost saving for a 100-aircraft LRSA fleet, the study determined that incorporation of SMART technology into the Mach 2.4 LRSA vehicle's inlets would produce a $769 million saving over conventional-bleed-equipped aircraft! The life-cycle cost saving was even greater for the Mach 4.0-class LRSA.

A further stage of this trade study addressed the potential payoff for SMART in a turbofan-engined Mach 2.4 LRSA vehicle. At this stage, the SMART benefit for the original PDE-

powered LRSA was re-evaluated (owing to impact of vehicle design evolution and slightly altered inlet-performance assumptions), and (as before) the vehicle was resized, etc. to reflect changes enabled by SMART. When all was said and done, the SMART-equipped, turbofan-powered Mach 2.4 LRSA showed 100-aircraft life-cycle $ savings (relative to conventional bleed) equivalent to the SMART-equipped, PDE-powered version: approximately $1.5 billion in both cases!